Third International Conference on CFD in the Minerals and Process Industries
CSIRO, Melbourne, Australia
10-12 December 2003

CFD MODELLING OF THE FLOW AND REACTIONS IN A FLASH FURNACE SMELTER REACTION SHAFT

Christopher B. SOLNORDAL[1], Frank R. A. JORGENSEN[1], Peter T. L. KOH[1], and Arthur HUNT[2]

[1] CSIRO Minerals, Clayton, Victoria 3169, AUSTRALIA
[2] WMC Resources Ltd – Olympic Dam Operations, South Australia, AUSTRALIA

ABSTRACT

The performance of flash furnace burners can be evaluated quickly and efficiently using CFD modelling. Gas flows are modelled using the conventional Eulerian approach, while Lagrangian particle tracking is used to model the flow of solid feed through the burner and into the reaction shaft. A Composite Particle Model has been developed that considers the solid feed to be made up of single particles containing appropriate quantities of concentrate, flux and dust. Solid fuels (such as coal) can also be included in the composite particle. Reactions between the solids and gas are then modelled using standard heat and mass transfer relationships. Results from the modelling process are shown for WMC's Olympic Dam copper flash smelter with the burner that was used from '98-'03. Flow patterns, temperature and gas composition distributions, particle dispersion and residence time, and overall extent of sulphur removal are predicted and used to evaluate furnace performance. However, results are sensitive to the assumed size of the composite particles, and plant measurements are required to determine the appropriate composite particle size to predict quantitative data.

INTRODUCTION

To accurately model the combustion processes taking place within a flash smelter it was necessary to develop a separate model of flash concentrate combustion that could be incorporated into the CFD packages in use at CSIRO Minerals. Initial development took place within the PHOENICS environment for nickel flash smelting (Koh and Jorgensen, 1994). CSIRO ported the model to CFX-4 and modified it to investigate zinc flash smelting (Koh *et al.,* 1997). The current work was undertaken in 1998-9 to investigate the capability of a new concentrate burner in WMC's Olympic Dam Operations (ODO) copper flash smelting shaft over a range of operating conditions. Thus the sub-model was further modified to simulate the combustion in the ODO copper flash smelting shaft. The burner modelled in this work was in operation from 1998 to early 2003. It has since been replaced by a new technology burner that operates at over 70 tph concentrate.

In this paper the combustion sub-model is presented, together with some results of the ODO smelter investigations, in particular the performance of the smelter under high flow rate and turn down conditions.

MODEL GEOMETRY

The modelling work was performed using the configuration of the burners as it was in 1999 (Figure 1) Concentrate, dust, flux and oxygen enriched air enter the reaction shaft through a central burner. Additional heat for combustion is provided by three oil burners positioned around the concentrate burner.

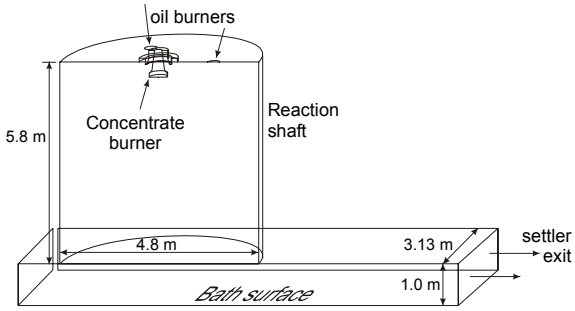

Figure 1: Schematic diagram of geometry.

The solids react with the oxygen in the reaction shaft, liquid metal and slag are deposited in the bath and gases and dust exit through the settler. The geometry was symmetrical about its longitudinal axis, and was modelled as a symmetric half-slice.

MATHEMATICAL MODEL FORMULATION

The problem was solved using CFX-4.1. Eulerian simulation was used for the gas phase, while Lagrangian particle tracking was used for concentrate particles and oil droplets. Model features included:-

- Steady state solution for momentum, energy and turbulence;
- Standard k-ε turbulence model (Launder and Spalding, 1974);
- Radiation using the Shah technique (Lockwood and Shah, 1980);
- Oil droplets were simulated using a total of 60 particle tracks;
- Concentrate particles were represented by a total of 1200 particle tracks.

Concentrate Combustion Submodel

CFX-4 did not allow the simultaneous tracking of concentrate particles and oil droplets, so individual tracking routines were developed by CSIRO Minerals. The concentrate combustion sub-model assumed all solid material (concentrate, flux and dust) entered the flow domain in single composite particles containing all components. The composite particle would then undergo a series of reactions, the speed of which depended on the temperature and composition of the particle, and the local gas composition. The sub-model was tailored to the

chemistry of the ODO flash furnace feed (see Table 1 and Table 2) In summary:-

- Particles heat up to 500 °C without reaction;
- Covellite (CuS), chalcopyrite ($CuFeS_2$) and pyrite (FeS_2) decomposes at 500 °C;
  - Labile sulphur from the decomposition reactions combusts with oxygen to form SO_2 at some distance from the particle, releasing heat to the gas phase, and particles ignite;
  - Some heat is transferred back to the particles. Since the reactions are endothermic, the decomposition rate is limited by this heat transfer;
  - The temperature remains constant at 500 °C until all CuS, $CuFeS_2$ and FeS_2 has decomposed;
- Particles continue to heat up to 670 °C;
- At 670 °C the bornite (Cu_5FeS_4), digenite ($Cu_{1.74}S$) and $CuSO_4$, and $CuFe_2O_4$ from the dust are assumed to decompose. Again liberated sulphur reacts with oxygen to form SO_2, and the temperature remains constant at 670 °C until the reactions are complete;
- Particles continue to heat up to 800 °C with no further reaction;
- At 800 °C the remaining minerals either react or decompose further;
  - In this case the reaction rate is controlled by oxygen diffusion to the particle surface;
  - The overall reaction is exothermic;
  - FeO and Cu are produced in the particle, with sulphur dioxide entering the gas phase.
- Once all oxygen in consumed, the reactions cease.

As a particle undergoes these reactions its mass and diameter are changing. The relationship between particle temperature and the fraction of sulphur removed from the particle is shown schematically in Figure 2.

	Concentrate			Dust	Flux
	Average grade	Low grade	High grade		
Cu:S	1.6	1.4	2.2	2.5	-
Cu (wt%)	45.9	41.3	55.6	35.8	
S (wt%)	28.7	29.7	24.8	14.4	
Fe (wt%)	20.1	23.4	15.6	13.7	0.8
SiO_2 (wt%)	3.1	3.1	2	2.6	93.0
Al_2O_3 (wt%)	0.6	0.6	0.6		
CaO (wt%)	0.1	0.1	0.1		
U_3O_8 (g/t)	250	250	250		
Other (wt%)				33.5	6.2

Table 1: Nominal feed compositions.

		Concentrate grade (wt%)		
		Average	Low	High
Chalcopyrite	$CuFeS_2$	40.18	54.75	8.43
Bornite	Cu_5FeS_4	31.32	21.42	39.98
Chalcocite	Cu_2S	0.00	0.00	17.6
Covellite	CuS	16.8	12.04	23.2
Pyrite	FeS_2	1.9	1.9	1.9
Hematite	Fe_2O_3	5.0	5.0	5.0
Silica	SiO_2	3.1	3.1	3.1
Copper	Cu	1.0	1.0	1.0
Lime	CaO	0.1	0.1	0.1
Alumina	Al_2O_3	0.6	0.6	0.6

Table 2: Mineralogical Composition of Concentrate.

Oil Combustion Submodel

The coding of the oil combustion submodel utilised the eddy break-up model resident in CFX4, but allowed simultaneous calculation of both oil and concentrate combustion (Koh 1996). Significant points to note are :-

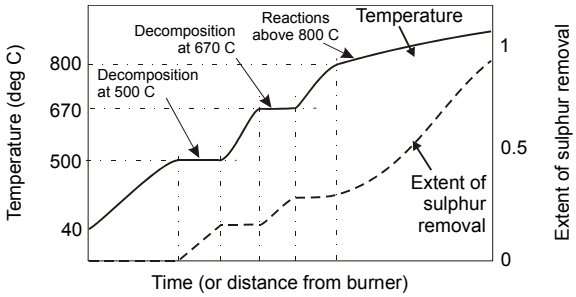

Figure 2: Idealised bahaviour of the composite particle during combustion.

- The oil vapour reaction rate is determined by the chemical kinetics in conjunction with the eddy-breakup combustion model;
- The forward reaction is modelled;
- The rate constant is determined from the Arrhenius equation;
- All heat from the reaction is released to the furnace in the products of combustion and by radiation and convection.

Boundary Conditions

Inlets

The concentrate and oil burners were modelled as Dirichlet boundaries. Velocity and temperature conditions are specified in Table 3. Turbulence quantities were estimated at the inlets using empirical functions of the inlet hydraulic diameter. Such estimates are valid for small inlets into a large flow domain.

Input stream	Inlet	Flow Rate	O_2 conc.	Temp. (°C)
Concentrate	Conc chute	70000 kg/hr	-	60
Dust	Conc chute	7000 kg/hr	-	45
Flux	Conc chute	5000 kg/hr	-	20
Chute gas	Conc chute		0.21	60
Combustion gas	Comb entry	33866 Nm^3/hr	0.5	40
Oil	Oil burner	80 l/hr/burner	-	60
Oil combustion gas	Oil burner	550.33 Nm^3/hr/burner	0.21	40

Table 3: Nominal inlet conditions to main flow streams.

Walls

All solid surfaces such as the shaft wall and roof were modelled as no-slip wall boundaries. The bath surface was also modelled as a wall boundary, since the motion of the bath was not significant compared to the gas flow. The shaft roof temperature was specified as 1000 °C, while the shaft and settler walls and bath surface had a temperature of 1500 °C. Some surfaces of the concentrate burner had a zero heat flux boundary condition, while the cooled components were held at a constant temperature of 40 °C.

Outlet

Only one outlet boundary was present in the geometry, which corresponded to the outflow through the settler. A constant pressure boundary condition was specified so that all gradients perpendicular to the boundary were zero.

RESULTS

The conditions under which simulations were performed are summarised in Table 4. Runs 1 and 2 use the same conditions summarised in Table 3, while Runs 3 and 4 use proportionately lower and higher rates of flow.

Run	Solids rate (tph) cons/flux/ dust	Cons grade	Tot O_2 flow rate (Normal m^3/hr)	Oil rate (l/hr/ burner)	Ptcle size (μm)
1	70/7/5	Ave	17500	80	30
2	70/7/5	Ave	17500	80	20
3	40/4/2	High	8857	300	30
4	100/10/9	Low	26673	0	30

Table 4: Inlet conditions for the 4 CFD runs.

Nominal Flow Conditions: Run 1

Reaction Shaft Flow Patterns

Figure 3 shows the velocity vector plot for Run 1 in the symmetry plane. The central jet is shown to spread only marginally as it travels down the reaction shaft, and recirculation zones are established on both sides of the jet. There is a slight displacement of the jet towards the settler, due to the flow exiting the shaft in that direction. The vector plot also shows the location of the oil burner in the symmetry plane, which joins the central jet of concentrate approximately 2-3 m down the reaction shaft.

Figure 4 shows a single slice through the reaction shaft, 0.8 m below the shaft roof. In this figure the horizontal and component of velocity is shown using vectors, while regions of rising and descending flow are shown using coloured contours. At this level in the shaft gases rise up the wall opposite the setter (left), then flow across the upper shaft region (black vectors) and descend slightly on the shaft wall nearest the settler (right). The flames from the two off-centre oil burners have been pushed in the direction of the settler by the bulk gas in the shaft, leading to the asymmetric location of the plume. Figure 5 shows an isosurface of constant velocity in the reaction shaft that further demonstrates this behaviour.

Temperature and Gas Composition Distributions

Figure 6 shows the distributions of temperature and O_2 in the symmetry plane, as well as the predicted particulate behaviour. Figure 6 (a) shows the temperature distribution in the furnace, and both the concentrate plume and oil jet is well defined. The oil flame is the hottest part of the furnace (1865 °C) while the centre of the concentrate jet remains relatively cool until it approaches the bottom of the reaction shaft. Concentrate therefore heats up (and reacts) from the outside of the jet. The cool region narrows as the bath surface is approached. However, it is predicted that temperatures below 600 °C prevail down the reaction shaft.

The volume concentration of O_2 is shown in Figure 6 (b). At the gas inlet the oxygen volume fraction is 0.5. The oxygen in the gas stream reacts with the concentrate and generates SO_2. Sufficient oxygen is supplied to the furnace to allow sulphur in the concentrate to completely combust. The far field oxygen concentration is zero indicating that all oxygen has been consumed and all sulphur has therefore been removed from the concentrate (Figure 6 (f)).

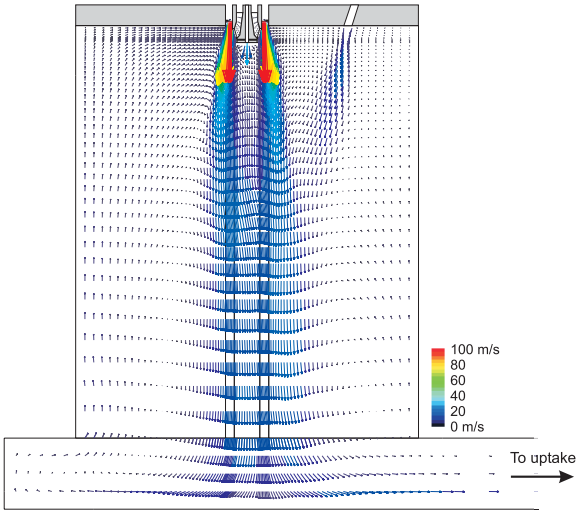

Figure 3: Velocity field in symmetry plane for Run 1.

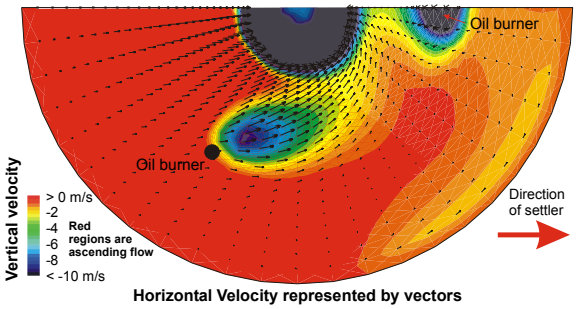

Figure 4: Full slice through the reaction shaft 0.8 m below the shaft roof, Run 1.

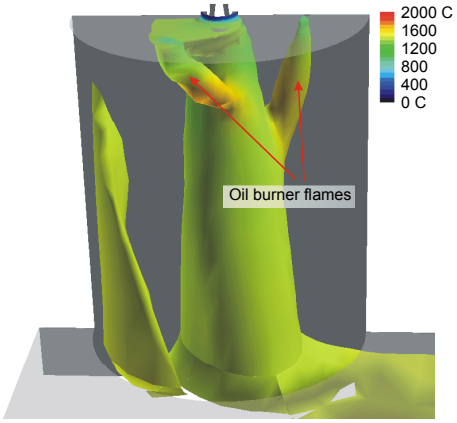

Figure 5: Isosurface of constant speed (7 m/s) coloured by temperature. Run 1.

Figure 6 (c) shows 200 of the 1200 concentrate particle tracks, colour-coded with the degree of sulphur removed from the particle. The concentrate particles only start to react as they move out of the cool region of the central

plume. Also, all of the particles end up completely reacted (red). Several of the particle tracks continue out the settler (as dust), while some recirculate within the reaction shaft. Calculation of the particle tracks took the greatest amount of computational time, and hence a time limit of 1.0 s was imposed on each track. Therefore, much of the particle recirculation in the shaft is not shown.

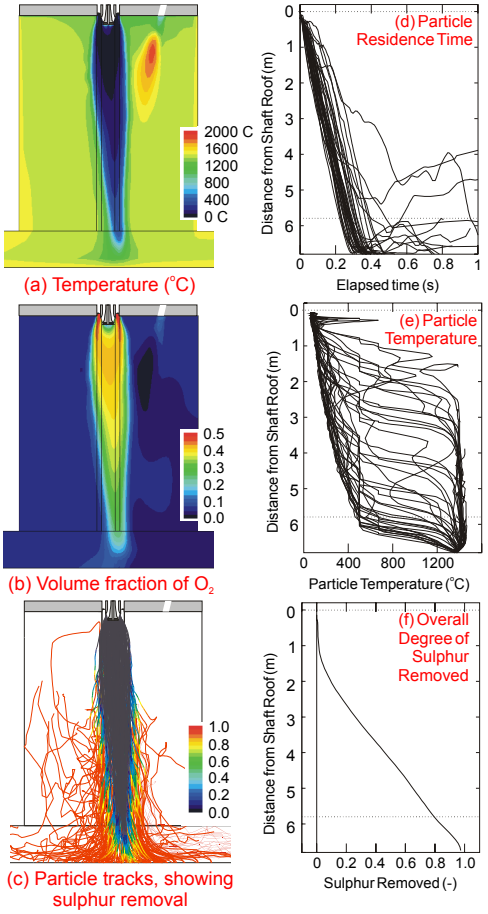

Figure 6: Temperature, and O_2 distributions for Run 1, together with concentrate particle characteristics.

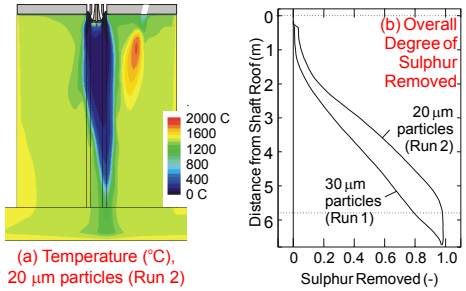

Figure 7: Temperature distributions and degree of sulphur removal for Runs 1 and 2.

Figure 6 (d) and (e) show characteristics of a selection of particle tracks as they travel down the reaction shaft. On each graph there are two horizontal dashed lines. The line at 0 m from the shaft roof represents the shaft roof itself, while the line at 5.8 m from the shaft roof represents the settler roof. The graphs end 6.8 m from the shaft roof, which is the level of the bath surface. Figure 6 (d) shows the particle elapsed time in the reaction shaft. Most particles have reached the bath surface within 0.25 and 0.50 s. Figure 6 (e) shows the temperature of particles as they travel down the reaction shaft. Each particle heats up relatively quickly once it starts to combust, and individual particles are shown to completely react within about 1 m once they commence reaction. However, the distribution of particle temperatures further indicates that it is the outside particles that react and not until they have reacted do the innermost particles get the opportunity to react.

Figure 6 (f) shows the average removal of sulphur from all concentrate particles. The total sulphur removed is predicted to be greater than 99%. However, this prediction is based on the assumption of concentrate particles having a constant initial diameter of 30 μm. The presence of larger particles will reduce the degree of reaction. Conversely, smaller particles will react faster than predicted.

Variation in Assumed Composite Particle Size: Run 2

The nominal conditions modelled in Run 1 assumed the composite particle to have a constant size of 30 μm. Little is known about the true particle size distribution of the solids feed and it is believed that much of the concentrate is agglomerated within the reaction shaft as it descends (Debrincat *et al.*, 2000; Debrincat, 2003). However, since the majority of the primary particles are less than 30 μm in diameter, it was decided to investigate the effect of decreasing the particle size to a constant value of 20 μm. The results are shown in Figure 7.

Figure 7 (a) shows the temperature distribution for Run 2. The concentrate plume is substantially shorter when using an assumed composite particle size of 20 μm (c.f. Figure 6 (a)), suggesting that the smaller particles are reacting faster. The low thermal mass of the smaller particles allows them to heat up and ignite quickly, while their greater surface area also increases reaction rate. The extent of reaction is shown in Figure 7 (b) for both Runs 1 and 2. The 20 μm particles allow the complete removal of sulphur from the concentrate within 5.5 m of the shaft roof, which is considerably faster than for the 30 μm particles.

Since the results predicted by the model are dependent on concentrate particle size and the actual size distribution is not accurately known, all data must be used for observing variational trends rather than absolute predictions of burner/shaft behaviour.

Variation in Feed Rate: Runs 3 and 4

Runs 3 and 4 investigated the effect of varying the feed rate of concentrate into the reaction shaft. As the rate of concentrate was changed, so too was the concentrate grade. At the lower concentrate rate a greater quantity of heat was required and consequently the flow rates to the oil burners were increased (Table 4). At the high concentrate rate the reaction was autogenous and the oil burners were turned off. Also, the oxygen flow rate through the concentrate burner was adjusted to allow complete combustion of the concentrate.

The temperature distributions in the reaction shaft for Runs 1, 3 and 4 are shown in Figure 8 (a) – (c). The temperature plume with 40 tph concentrate (Run 3, Figure 8 (a)) is substantially smaller than for 70 tph concentrate (Run 1, Figure 8 (b)). Also, the oil flame is hotter and longer, and the reaction shaft is slightly higher in temperature. The temperature profile for 100 tph concentrate (Run 4, Figure 8 (c)) is considerably cooler and the concentrate plume jets rapidly to the bath surface.

The model predicts the combustion gas to jet towards the bath surface without heating up above 200 °C. Such behaviour may cause an accumulation of solid concentrate on the bath surface, and even local freezing of the bath.

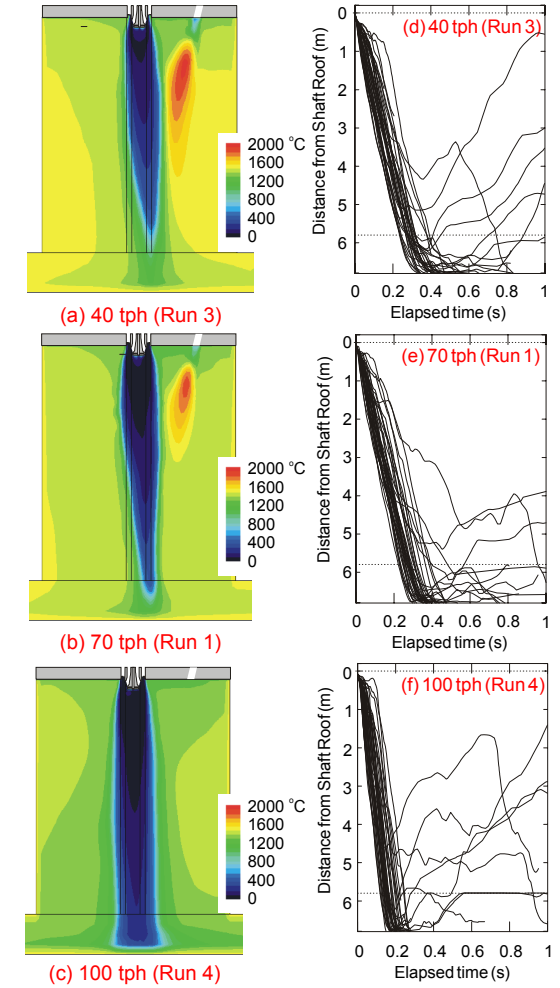

Figure 8: Temperature distributions and particle residence times for Runs 3, 1 and 4.

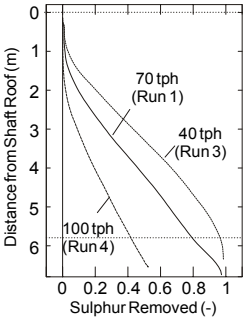

Figure 9: Extent of reaction for Runs 1, 3 and 4.

The extent of reaction as a function of distance below the shaft roof is shown in Figure 9 for the three concentrate feed rates, and the poor extent of reaction at 100 tph is shown. At 40 tph concentrate rate the entire feed is fully reacted by approximately 6 m below the shaft roof. For the nominal flow rate of 70 tph the concentrate can nearly fully react by the time the concentrate reaches the bath surface. However, at 100 tph concentrate less than 60% of the concentrate has reacted before hitting the bath surface.

Figure 8 (d) - (f) shows the residence time of particles under the three conditions of concentrate feed rate. There is only a small difference in residence time between the 40 tph and 70 tph feed rates, each being approximately 0.3 – 0.5 s. However, at 100 tph the residence time of most particles is significantly smaller at 0.2 – 0.3 s. This result suggests that the initial velocity of the combustion gas, as well as the flow rate of gas and solids, controls the residence time of the concentrate particles.

DISCUSSION

Variation in Concentrate Particle Size

The concentrate particle size has a significant effect on the rate of reaction occurring in the reaction shaft. This is because the reaction rate is dependent on the surface area available for heat transfer and reaction between gas and solid, and small particles have a significantly greater surface area per unit mass of concentrate.

Although particle size distributions can be measured for a given sample of concentrate, the distribution will depend greatly on the conditions under which it is measured. Furthermore, the presence of flux and dust in the feed will alter the distribution, especially flux which has an average particle size one order of magnitude greater than the concentrate and dust. Jorgensen (1987) has shown that agglomerates may exist in the shaft due to poor dispersion of concentrate, while Debrincat *et al.* (2000) and Debrincat (2003) have demonstrated the high propensity of flash furnace concentrate to resist dispersion even in a highly turbulent dispersing environment. Thus it is difficult to give an estimate of the particle size distribution of the feed stream entering the reaction shaft, or indeed specify how that distribution may vary in the shaft.

Another unknown in the estimation of particle size distribution is the effect of the assumed distribution on the destination of the concentrate particles. If all particles are assumed to be extremely small then they will likely be carried out of the furnace in the off-gases, even if they are completely reacted.

At this stage the distribution of concentrate particle size in the reaction shaft it is probably the biggest unknown in the flash furnace modelling problem, and given the number of variables governing its value, a constant value for composite particle size of 30 µm was considered the best approach. By decreasing this to 20 µm it was possible to gauge the amount of change the assumed particle size has on the predicted results.

As shown in Figure 7, the size of the combustion region beneath the burner was significantly reduced when a particle size of 20 µm was assumed. Also, the same quantity of concentrate was fully reacted approximately 1.5 m further up the reaction shaft when assuming the smaller particle size. These results give an indication of how sensitive the predicted furnace behaviour is to the assumed composite particle size, and it is recommended that plant measurements be taken in order to tune this parameter so that quantitative results can be obtained.

Variation in Concentrate Feed Rate

Runs 3 and 4 demonstrated the effect of varying the concentrate feed rate. At the low feed rate it was possible for all the sulphur to be removed from the concentrate within the reaction shaft (Figure 9). The results indicate that concentrate is not spread more efficiently at lower

flow rates and the gas-solid contact is approximately the same for all three runs. However, the residence time of concentrate is greater at the lower feed rates (Figure 8), which would allow particles more time to fully react.

The predicted behaviour for Run 4 suggests that the furnace would not run at feed rates of 100 tph. Furthermore, at 70 tph concentrate feed rate there is only just enough height in the shaft to allow full sulphur removal, suggesting that any increase in feed rate will result in decreased efficiency.

One aspect of the high feed rate case (Run 4) that may limit performance is that the gas velocity through the burner had to be increased to 153 m/s (from 100 m/s) to allow enough gas into the furnace. Figure 8 (f) shows that the high velocity reduces the residence time of the concentrate, which consequently limits the extent of reaction.

Model Limitations

As with all mathematical models, the predictions of the model are only as good as the assumptions made in modelling the process. In the current work several limitations were identified with the methods used, the most significant of which is the assumed composite particle size distribution (which has already been discussed). Other points to consider are:

- **Wall Boundary Conditions.** All furnace walls were assumed to have constant temperatures. In some simulations (Figure 8 (c), for example) the furnace and settler walls are clearly at a higher temperature than the gas, and the assumption of constant temperature walls is invalid. A better modelling approach would be to use furnace jacket heat losses to specify a heat flux boundary condition at the wall.
- **Bath Surface Boundary Conditions**. Similar problems occurred from specifying the bath surface to be at a constant temperature of 1500 °C. Again Figure 8 (c) provides an extreme example where cool gases (approximately 200 °C) from the concentrate burner are predicted to jet onto the bath surface, but the gas temperature artificially elevates as it approaches the bath surface. An accurate model of the transfer of heat away from this localised surface would be complex.
- **High Solids Loading Around the Burner**. The solid particles are tracked through the gas using a Lagrangian approach. One assumption of this approach is that the concentration of solids is negligible. However, in the high solids region and around the solids chute this assumption is not valid. It was therefore not possible to simulate the flow within the solids chute, and the initial velocity of solids at the exit was determined experimentally.

CONCULSIONS

The CSIRO flash furnace concentrate combustion sub-model has been successfully applied to the copper flash furnace at ODO. The flow field and reactions occurring within the reaction shaft have been simulated. The following observations were made:

- Flow patterns under nominal operating conditions of 70 tph concentrate are not axisymmetric in the reaction shaft. The central jet is displaced toward the settler exit, as are the flames from the oil burners. The region of concentrate combustion is confined to the central jet of combustion gas, and is kept well away from shaft walls.
- The predicted reaction behaviour is strongly affected by the solids particle size that is assumed.

Assuming a composite particle size is constant at 30 μm:

- Solids feed rate greatly affects the performance of the furnace, both in terms of degree of sulphur removal and furnace temperature. At a concentrate feed rate of 40 tph all sulphur is predicted to be removed from the concentrate, whereas at 100 tph only 60% of the sulphur is removed and plume temperatures drop. Large quantities of unreacted concentrate and cool gas jet onto the surface of the bath.
- The furnace height is just adequate to allow full removal of sulphur at a feed rate of 70 tph, and any increase in feed rate will lead to decreased burner/shaft performance.

ACKNOWLEDGMENTS

The assistance of Phil Schwarz (CSIRO Minerals), and Greg Hill, Simon Cmrlec and Ilija Sutalo (ODO) is gratefully acknowledged. Financial support for this work was provided by WMC Resources Ltd. Permission to publish this work was granted by CSIRO Minerals and ODO, and is gratefully acknowledged.

REFERENCES

DEBRINCAT, D.P., 2003. "Disintegration of Powder Agglomerates in a Flash Furnace Shaft", PhD Thesis, University of Melbourne, Melbourne, Vic., Australia.

DEBRINCAT, D.P., SOLNORDAL, C.B., VAN DEVENTER, J., JORGENSEN, F.R.A. and KOH, P.T.L., 2000. "Towards Understanding the in Situ Agglomeration of Nickel Concentrate Powder During Flash Furnace Injection", *Proceedings 1st Asian Particle Technology Symposium,* Bangkok, Thailand, 13-15 December 2000.

JORGENSEN, F.R.A., 1987. "Investigation of Shaft Reactions in Nickel Flash Smelting at 0.5 kg/min Scale", *Pyrometallurgy '87*, 21-23 Sept. 1987, Institution of Mining and Metallurgy, London, UK, pp. 263-287.

KOH, P.T.L. and JORGENSEN, F.R.A, (1994), "Modelling Particulate Flow and Combustion in a Flash Smelter", *In CHEMECA '94, Proceedings of the 22nd Australian Chemical Engineering Conference*, Perth, WA, Australia, pp. 499-506.

KOH, P.T.L., NGUYEN, T.V. and JORGENSEN, F.R.A, (1997), "Numerical Modelling of Combustion in a Zinc Flash Smelter", *In Proc. Int. Conf. On CFD in Mineral and Metal Processing and Power Generation*, Melbourne, Vic., Australia, 3-4 July 1997, pp. 205-211.

LAUNDER, B.E. and SPALDING, D.B., 1974. "The Numerical Computation of Turbulent Flows". *Comp. Meths. Appl. Mech. Engng.,* 3, pp. 269-289.

LOCKWOOD, F.C. and SHAH, N.G., 1980. "A New Radiation Solution Method for Incorporation in General Combustion Predictions Procedures". *Proceedings of the 18th Symposium (Int.) on Combustion, The Combustion Institute,* pp. 1405-1414.